

See discussions, stats, and author profiles for this publication at: <https://www.researchgate.net/publication/321162099>

Justification of design and parameters of Bernoulli–vacuum gripping device

Article in *International Journal of Advanced Robotic Systems* · November 2017

DOI: 10.1177/1729881417741740

CITATIONS

0

READS

7

4 authors:



Roman Mykhailyshyn

Ternopil Ivan Pul'uj National Technical Unive...

8 PUBLICATIONS 6 CITATIONS

SEE PROFILE



Volodymyr Savkiv

Ternopil Ivan Pul'uj National Technical Unive...

8 PUBLICATIONS 6 CITATIONS

SEE PROFILE



František Duchoň

Slovak University of Technology in Bratislava

64 PUBLICATIONS 151 CITATIONS

SEE PROFILE



Olena Fendo

Kyiv International University

2 PUBLICATIONS 2 CITATIONS

SEE PROFILE

Some of the authors of this publication are also working on these related projects:



Simulation orientation bernoulli gripping device with a displaced center of mass object manipulation

[View project](#)



Innovative HRI methods for robots' control in the real environment [View project](#)



Justification of design and parameters of Bernoulli–vacuum gripping device

Volodymyr Savkiv¹, Roman Mykhailyshyn¹,
Frantisek Duchon² and Olena Fendo³

Abstract

The dynamics of the air flow between interacting surfaces of Bernoulli–vacuum gripping device and object of manipulation is analysed. The methods of increasing lifting capacity in given devices are presented. The equation for defining pressure distribution in between interacting surfaces of gripping device and object of manipulation and equations for calculation of power characteristics is calculated. The results of theoretical researches of Bernoulli–vacuum gripping devices with different forms of active surfaces are introduced.

Keywords

Bernoulli–vacuum gripping device, object of manipulation, air flow, radial clearance, nozzle

Date received: 24 August 2017; accepted: 12 October 2017

Topic: Special Issue – Mobile Robots
Topic Editor: Andrey V Savkin
Associate Editor: Michal Kelemen

Introduction

When solving problems of automation of machined parts handling on certain machines and transfer lines, non-contacting pneumatic grippers are becoming more widely used.¹ Their specific feature is high reliability and durability, low production price, non-contacting grip and holding the objects of manipulation (OM), blanks and parts regardless of their material, mechanical characteristics, surface layer structure and temperature.

Non-contacting pneumatic grippers of industrial robots and manipulators have a range of advantages. However, there are no detailed theoretical and experimental researches in this area, which would lead to the creation of grippers with bigger carrying capacity, reliability in work and high speed of response. The analysis of scientific papers^{2–4} shows that the issue of improving the design of non-contacting pneumatic grippers aimed at providing high performance is of a low priority. The last fact is also confirmed by the analysis of designs and characteristics of Bernoulli gripping devices (BGDs), which are produced by famous foreign corporations (Bosch Rexroth, Schmalz, SMC Pneumatics, Festo).^{5–8} The

Mechatronic Systemtechnik GmbH works on the design of Bernoulli–vacuum gripping devices that combine Bernoulli principle and vacuum grippers.⁹ Also, a similar principle of work is proposed in the article.^{10,11} In an earlier work,¹² the values of the optimal outer diameter for a range of supply mass flow rates were calculated. In another work,¹³ a flexible, multifunctional gripper for handling variable size, shape and weight of unpacked food products is discussed.

A study by Dini et al.¹⁴ proposes the use of contactless grippers instead of more traditional vacuum cups or

¹ Department of Industrial Automation, Ternopil Ivan Pul'uj National Technical University, Ternopil, Ukraine

² Department of Robotics, Slovak University of Technology in Bratislava, Bratislava, Slovak Republic

³ Department of Computer Science, Kyiv International University, Kyiv, Ukraine

Corresponding author:

Roman Mykhailyshyn, Ternopil Ivan Pul'uj National Technical University, Ruska 56, Ternopil 46001, Ukraine.

Email: mykhailyshyn@tntu.edu.ua



Creative Commons CC BY: This article is distributed under the terms of the Creative Commons Attribution 4.0 License

(<http://www.creativecommons.org/licenses/by/4.0/>) which permits any use, reproduction and distribution of the work without further permission provided the original work is attributed as specified on the SAGE and Open Access pages (<https://us.sagepub.com/en-us/nam/open-access-at-sage>).

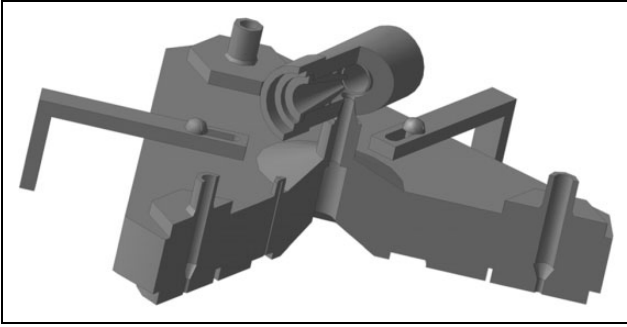


Figure 1. General view of Bernoulli–vacuum gripping device.

fingered grippers. In particular, the main objectives of this investigation are to measure the performance of different gripper configurations whose lifting force is generated by a high-speed air flow passing between the gripper and the leather ply and to analyse the dynamics of air flow in ejector and in between interacting surfaces of Bernoulli–vacuum gripping device and OM that defines the methods of increasing lifting capacity in given devices. This work also presents mathematical models, analyses force characteristics of Bernoulli–vacuum gripping devices with different forms of active surfaces and explains the choice of the most reasonable designs.

Design and operating principle of Bernoulli–vacuum gripping device

In comparison with vacuum gripping devices, the specific features of Bernoulli devices are high reliability and durability, objects' locating accuracy and high dynamic characteristics. The disadvantages of given devices are low force characteristics.

In comparison with Bernoulli devices of the same discharge characteristics, given Bernoulli–vacuum gripping device for flat OM (Figures 1 and 2) has 2.5 to 4 times higher carrying capacity. Besides, given device does not have any important drawbacks, which are usual for vacuum gripper devices.

Hard suction cup 1 with suction hole 2 and through-hole 3, where ejector body 5 is added using connector adapter 4, is used in given device. Ejector body consists of nozzle 6 and bushing 7. Created reception chamber 8 is connected to the suction hole 2 via through-hole 3. Three Bernoulli grippers 9 are installed on the periphery of hard suction cup 1. Flat butt end surfaces of the grippers 9 are on the same flat surfaces, and their axes are placed within certain radius and radial space is the same. Also, the butt end surfaces of the grippers 9 are displaced from the surfaces' butt end of the suction cup 1 so that $h_0 - h_1 = 0.03/0.05$ mm.

The principle of this gripping device is as follows: during the supply of the compressed air from pneumatic system to the nozzle 6, negative pressure is produced in chamber 8 by means of ejection, and the air is sucked from the suction hole 2 via through-hole 3, which results in the area of low pressure. Air flows from BGD nozzle 9, which

are directed to the OM 10, influence on it with viscous friction and reactive repulsion force. When reducing the space h_1 between flat surfaces of BGD and OM to smaller than 0.5 mm, suction of air flow increases and prevails reactive force. When reducing space 11, the negative pressure increases in suction hole 2 of the suction cup. As a result, the object moved in the direction of the butt end of gripper. In case $h_0 < 0.04$ mm, negative pressure in suction hole 2 reaches the maximum level, and resilient pneumatic cushion between flat surfaces of BGD and OM is created.

By keeping the difference of atmosphere pressure and absolute pressure in the suction hole 2, the OM 10 is directly connected to suction cup surface butt end 1, as it is balanced by resilience of pneumatic cushions. The OM fixing from shift in a horizontal plane is made by expense of the supports 12.

Depending on structural design (Figure 3), hard suction cup 1 provides different operational characteristics (distance of OM gripping, maximum lifting force at optimal distance between gripper and OM, etc.). The solid flat surface of hard suction cup (Figure 3(a)) provides OM gripping from long distance. The shift between surface butt ends of the suction cup for δ (Figure 3(b) and (d)) or the use of capillary tube restrictor 13 in suction cup design (Figure 3(e)) provides opportunity of OM non-contact holding, even without the use of BGD. The presence of radial groove 14 in suction cup design (Figure 3(c) to (e)) provides increasing lifting force.

Despite the fact that restraining force of Bernoulli–vacuum gripping device is generally defined with suction cup lifting capacity, the use of Bernoulli devices in their design will improve dynamic characteristics, provide objects' gripping from larger distance and their non-contact holding.

Defining lifting force of gripping device

In general, lifting force of Bernoulli–vacuum gripping device of flat object is as follows

$$F = F_1 + 3F_2 \quad (1)$$

where F_1 is the force which appears as a result of impact on OM by difference of atmospheric pressure and absolute pressure in zone opposite to suction cup 1 ($0 < r < r_3$); F_2 is the force which appears as a result of impact of one BGD.¹⁵

The lifting force which is derived from vacuum suction cup (Figure 3(e)) is as follows

$$F_1 = \pi r_0^2 (p_a - p_1) + 2\pi \int_{r_0}^{r_1} (p_a - p_{r1}) r dr + \pi (r_2^2 - r_1^2) (p_a - p_2) + 2\pi \int_{r_2}^{r_3} (p_a - p_{r2}) r dr \quad (2)$$

where p_{r1} and p_{r2} are the functions of air absolute pressure distribution in radial clearance according to the zones

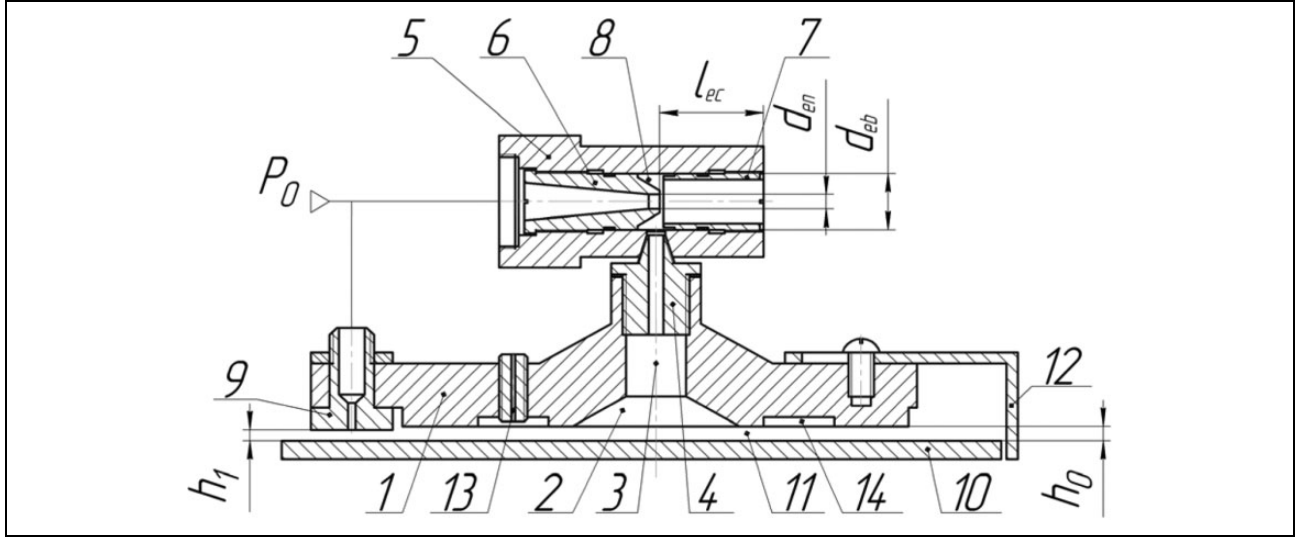


Figure 2. Principal scheme of Bernoulli–vacuum gripping device.

$r_0 < r < r_1$ and $r_2 < r < r_3$; p_1 is the absolute pressure created by ejector in the suction hole 2; p_2 is the absolute pressure in radial groove 14; p_a is the atmospheric pressure; r_0, r_1, r_2 and r_3 are the radii of the suction cup surface butt ends.

To define absolute pressure p_1 , the equation of force impulse for nozzle outlet section 6 and ejector bushing 7 should be comprised

$$G_e V_e + G_\Sigma V_{oc} + p_1 S_{eb} - (G_e + G_\Sigma) V_{ob} - p_a S_{eb} - F_f = 0 \quad (3)$$

where G_e and V_e are mass air flow and air velocity coming out from the nozzle 6; $G_\Sigma = G_1 + G_2$ is the total mass air flow which is sucked by ejector from atmosphere via radial clearance in zone $r_2 \leq r \leq r_3$ (G_1) and restrictor 13 (G_2); V_{oc} is the gripped air flow velocity at the out of suction ejector chamber 8; V_{ob} is the air flow velocity at the out of suction ejector body; $S_{eb} = \pi d_{eb}^2 / 4$ is the area of suction ejector body; d_{eb} is the diameter of suction ejector body; F_f is the friction force of air flow to the walls of suction ejector chamber.

On the basis of the flow continuity equation and ideal gas law, the velocity of gripped air flow at the in of ejector chamber 8 is defined as follows

$$V_{oc} = \frac{4G_\Sigma RT_a}{\pi(d_{eb}^2 - d_{en}^2)p_1} \quad (4)$$

where $R = 287.14 \text{ J}/(\text{kg} \cdot \text{K})$ is the gas constant for air; T_a is the absolute temperature of air flow in ejector mixing chamber which is approximately equal to the environmental temperature; d_{en} is the diameter of ejector nozzle.

Air flow velocity at the out of suction ejector chamber is defined as follows

$$V_{ob} = \frac{G_e + G_\Sigma}{S_{eb}\rho_a} \quad (5)$$

where ρ_a is the air density at the out of suction ejector chamber which is equal to atmospheric one.

Friction force of air flow to the walls of suction ejector chamber¹⁶

$$F_f = \pi \lambda_e l_{ec} d_{eb} \frac{(G_e + G_\Sigma)^2}{8\rho_a S_{eb}^2} \quad (6)$$

where λ_e is the average coefficient value of viscous friction to the inner walls of ejector chamber;¹⁶ l_{ec} is the ejector chamber length.

Taking into consideration above-mentioned dependences, the following equation will be received

$$G_e V_e + \frac{4G_\Sigma^2 RT_a}{\pi(d_{eb}^2 - d_{en}^2)p_1} - (p_a - p_1)S_{eb} - \frac{(G_e + G_\Sigma)^2}{S_{eb}\rho_a} \left(1 + \frac{\lambda_e l_{ec}}{2d_{en}}\right) = 0 \quad (7)$$

Mass air flow and velocity of supersonic flow through the nozzle 6 are defined using Saint-Venant-Vantsel equations for supercritical outflow mode¹⁷

$$G_e = \mu_{en} \frac{\pi d_{en}^2}{4} p_0 \sqrt{\frac{2}{RT_a} \frac{k}{k+1} \left(\frac{2}{k+1}\right)^{\frac{2}{k-1}}} \quad (8)$$

$$V_{en} = \varphi_{en} \sqrt{2RT_a \frac{k}{k-1} \left[1 - \left(\frac{p_1}{p_0}\right)^{\frac{k-1}{k}}\right]} \quad (9)$$

where $\mu_{en} = \varphi_{en} \varepsilon$ is the air flow coefficient via ejector nozzle;¹⁶ φ_{en} is the velocity coefficient; ε is the air contraction coefficient in the nozzle; p_0 is the absolute air pressure at the in of ejector; $k = 1.4$ is the adiabatic exponent of the air.

In order to define mass flow of G_1 and G_2 and air pressure distribution in p_{r1} and p_{r2} radial clearance, let's

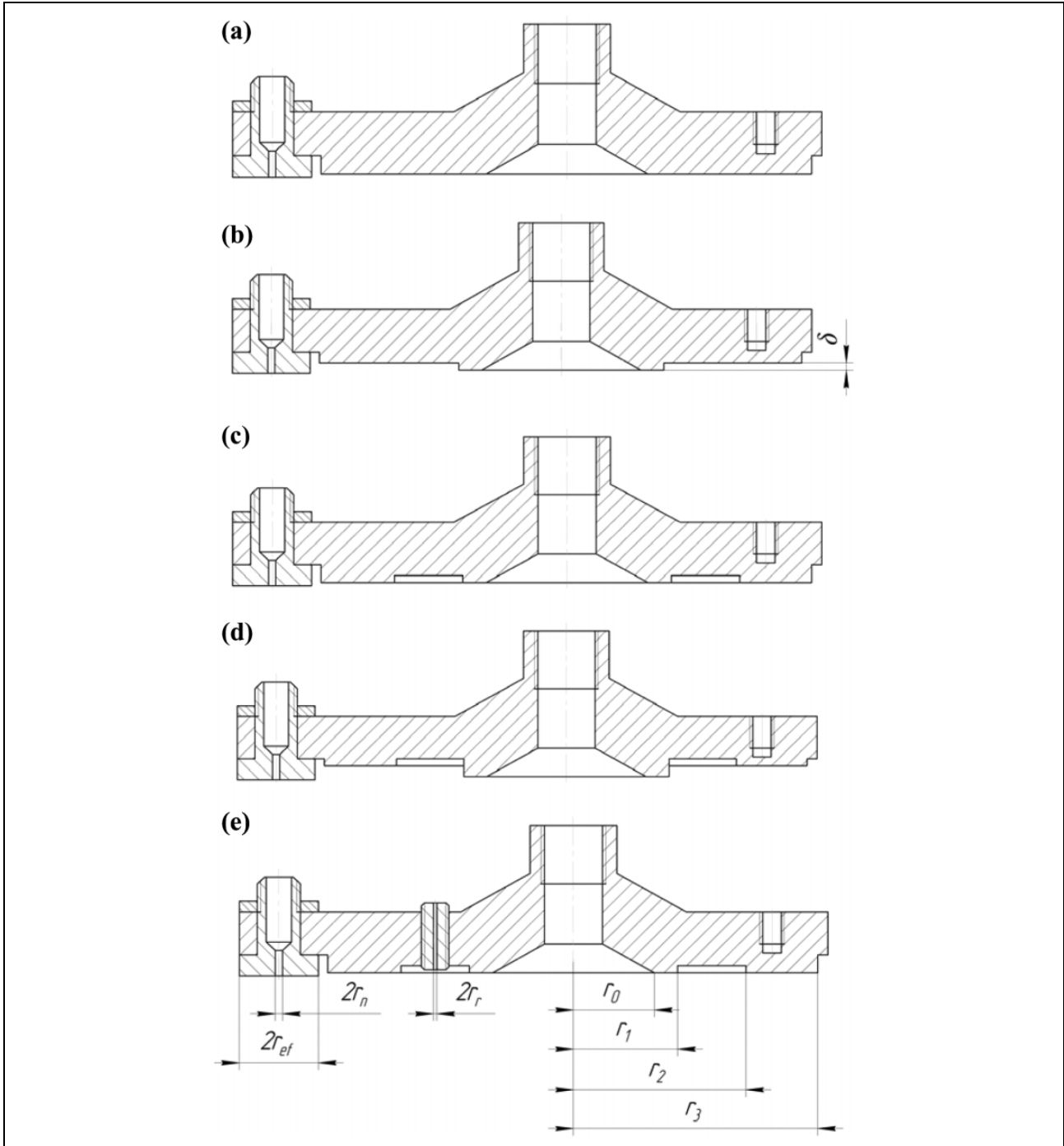


Figure 3. Constructions variants of the suction cup.

suppose that air flow velocity in radial clearance and capillary tube restrictor 13 is small, that is why these flows are considered to be laminar flows; air volume force is smaller than the pressure and friction force; thermodynamic process of air flow in radial clearance is considered to be isothermic; flat radial air flow motion is considered to be stable.

According to the study,¹⁸ the mass air flow in radial clearance may be defined as follows

$$G = \frac{\pi h_0^3}{6\mu_d RT_a} \frac{r}{dr} p_r dp_r \tag{10}$$

where $\mu_d = 1.71 \times 10^{-5} + 4.94 \times 10^{-8}t$ (kg/(s×m)) is the coefficient of air dynamic viscosity.

Taking into consideration flow continuity condition $G = \text{constant}$ in any section, the following equations will be right

$$\begin{aligned}
G_1 \int_{r_3}^{r_2} \frac{dr}{r} &= \frac{\pi(h_0 + \delta)^3}{6\mu_d RT_a} \int_{p_a}^{p_2} p_{r2} dp_{r2} \\
G_\Sigma \int_{r_1}^{r_0} \frac{dr}{r} &= \frac{\pi h_0^3}{6\mu_d RT_a} \int_{p_2}^{p_1} p_{r1} dp_{r1}
\end{aligned} \tag{11}$$

their solutions will be the equations for defining mass air flow

$$\begin{aligned}
G_1 &= \frac{\pi(h_0 + \delta)^3 (p_a^2 - p_2^2)}{12\mu_d RT_a \ln \frac{r_3}{r_2}} \\
G_\Sigma &= \frac{\pi h_0^3 (p_2^2 - p_1^2)}{12\mu_d RT_a \ln \frac{r_1}{r_0}}
\end{aligned} \tag{12}$$

When integrating equation (11) this way

$$G_\Sigma \int_{r_1}^r \frac{dr}{r} = \frac{\pi h_0^3}{6\mu_d RT_a} \int_{p_2}^{p_{r1}} p_{r1} dp_{r1}, \quad G_1 \int_{r_3}^r \frac{dr}{r} = \frac{\pi(h_0 + \delta)^3}{6\mu_d RT_a} \int_{p_a}^{p_{r2}} p_{r2} dp_{r2}$$

taking into account equation (12), pressure distribution functions in radial clearance will be received

$$\begin{aligned}
p_{r1} &= \sqrt{p_2^2 - \frac{p_2^2 - p_1^2}{\ln \frac{r_1}{r_0}} \ln \frac{r_1}{r}} \\
p_{r2} &= \sqrt{p_a^2 - \frac{p_a^2 - p_2^2}{\ln \frac{r_3}{r_2}} \ln \frac{r_3}{r}}
\end{aligned} \tag{13}$$

The mass air flow G_2 , which is sucked from the atmosphere via capillary tube restrictor 13 in radial groove 14, may be defined using the equation¹⁷

$$G_2 = \frac{\pi d_c^4 (p_a^2 - p_2^2)}{256\mu_d RT_a b} \tag{14}$$

where d_c and b are diameter and length of capillary tube restrictor, respectively.

Taking into consideration that $G_\Sigma = G_1 + G_2$, we'll get

$$\frac{\pi h_0^3 (p_2^2 - p_1^2)}{12\mu_d RT_a \ln \frac{r_1}{r_0}} = \frac{\pi(h_0 + \delta)^3 (p_a^2 - p_2^2)}{12\mu_d RT_a \ln \frac{r_3}{r_2}} + \frac{\pi d_c^4 (p_a^2 - p_2^2)}{256\mu_d RT_a b} \tag{15}$$

from which

$$p_2^2 = \frac{p_a^2 \left(\frac{(h_0 + \delta)^3}{3 \ln(r_3/r_2)} + \frac{d_c^4}{64b} \right) + p_1^2 \frac{h_0^3}{3 \ln(r_1/r_0)}}{\frac{(h_0 + \delta)^3}{3 \ln(r_3/r_2)} + \frac{d_c^4}{64b} + \frac{h_0^3}{3 \ln(r_1/r_0)}} \tag{16}$$

$$G_\Sigma = \frac{\pi h_0^3 p_1^2}{12\mu_d RT_a \ln(r_1/r_0)} \left(\frac{p_a^2 \left(\frac{(h_0 + \delta)^3}{3 \ln(r_3/r_2)} + \frac{d_c^4}{64b} \right) + \frac{h_0^3}{3 \ln(r_1/r_0)}}{\frac{(h_0 + \delta)^3}{3 \ln(r_3/r_2)} + \frac{d_c^4}{64b} + \frac{h_0^3}{3 \ln(r_1/r_0)}} - 1 \right) \tag{17}$$

After substituting equations (17), (8) and (9) in (7) and after transforming them, we will receive the equation from which absolute pressure p_1 in ejector chamber will be defined using numerical methods

$$\begin{aligned}
&1.4229\mu_{en}^2 d_{en}^2 p_0 \left(1 - \left(\frac{p_1}{p_0} \right)^{0.1429} \right) - \frac{\pi d_{en}^2}{4} (p_a - p_1) \\
&+ \frac{\pi h_0^6 p_1^3}{36\mu_d^2 RT_a (d_{eb}^2 - d_{en}^2) (\ln(r_1/r_0))^2} \left(\frac{p_a^2 \left(\frac{(h_0 + \delta)^3}{3 \ln(r_3/r_2)} + \frac{d_c^4}{64b} \right) + \frac{h_0^3}{3 \ln(r_1/r_0)}}{\frac{(h_0 + \delta)^3}{3 \ln(r_3/r_2)} + \frac{d_c^4}{64b} + \frac{h_0^3}{3 \ln(r_1/r_0)}} - 1 \right)^2 \\
&- \frac{4 + \frac{2\lambda_e l_{eb}}{d_{eb}}}{\pi \rho_a d_{eb}^2} \left(\frac{0.5378\mu_{en} d_{en}^2 p_0}{\sqrt{RT_a}} + \frac{\pi h_0^3 p_1^2}{12\mu_d RT_a \ln(r_1/r_0)} \left(\frac{p_a^2 \left(\frac{(h_0 + \delta)^3}{3 \ln(r_3/r_2)} + \frac{d_c^4}{64b} \right) + \frac{h_0^3}{3 \ln(r_1/r_0)}}{\frac{(h_0 + \delta)^3}{3 \ln(r_3/r_2)} + \frac{d_c^4}{64b} + \frac{h_0^3}{3 \ln(r_1/r_0)}} - 1 \right) \right)^2 = 0
\end{aligned} \tag{18}$$

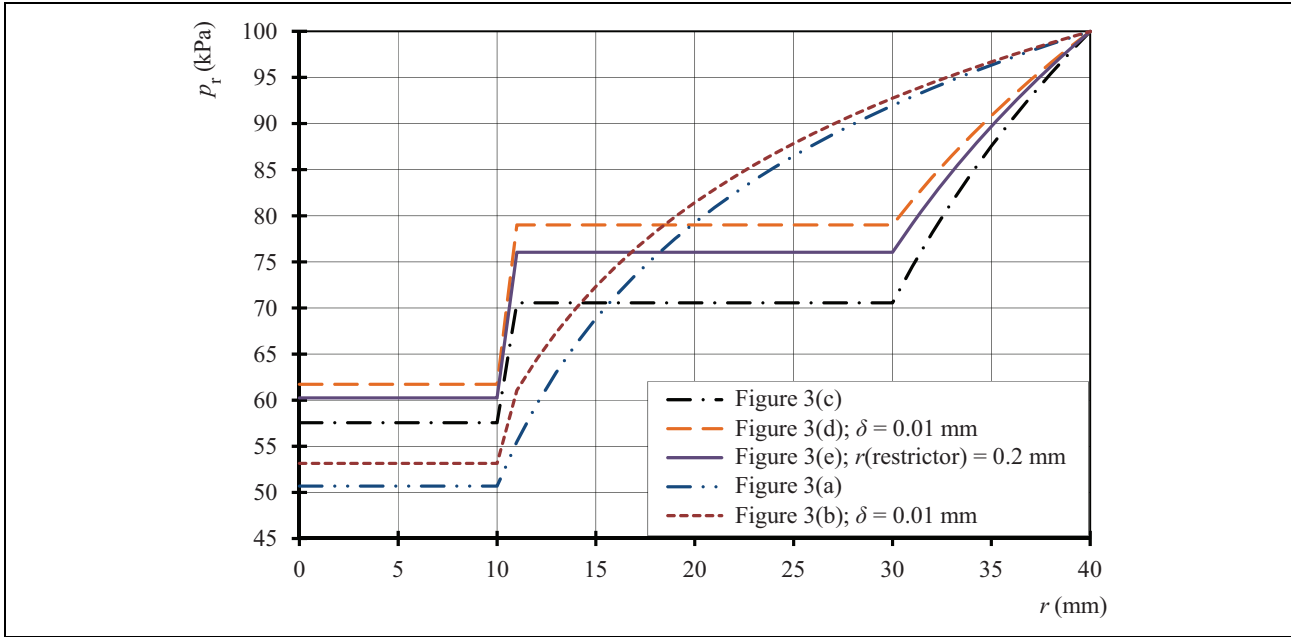


Figure 4. Negative pressure distributions on the surface of object manipulation, which are formed by different types of suction cups ($p_{0\text{ex}} = 200$ kPa; $h_0 = 0.04$ mm).

As a result, force F_1 will be shown in integral

$$\begin{aligned}
 F_1 = & \pi r_0^2 (p_a - p_1) + \pi (r_2^2 - r_1^2) (p_a - p_2) \\
 & + 2\pi \int_{r_0}^{r_1} \left(p_a - \sqrt{p_2^2 - \frac{p_2^2 - p_1^2}{\ln \frac{r_1}{r_0}} \ln \frac{r_1}{r}} \right) r dr \\
 & + 2\pi \int_{r_2}^{r_3} \left(p_a - \sqrt{p_a^2 - \frac{p_a^2 - p_2^2}{\ln \frac{r_3}{r_2}} \ln \frac{r_3}{r}} \right) r dr
 \end{aligned} \quad (19)$$

the solution of which is found using approximate approach, after previously calculating the value of p_1 and p_2 using dependences (18) and (16).

Justification of the gripping device surface parameters

The research of influence of power supply parameters and Bernoulli–vacuum gripping device design parameters on their operational characteristics was done using above-mentioned method. The calculations have been conducted for different values of excess pressure $p_{0\text{ex}} = p_0 - p_a$ and different types of suction cups with the following parameters: $r_0 = 10$ mm, $r_1 = 11$ mm, $r_2 = 30$ mm, $r_3 = 40$ mm, $d_{\text{en}} = 1.5$ mm, $d_{\text{eb}} = 3$ mm, $l_{\text{eb}} = 10$ mm, $\mu_{\text{en}} = 0.92$ and $\lambda_{\text{eb}} = 0.035$. The negative pressure distributions, which are formed by different types of suction cups, on the OM surface are presented in Figure 4. The graphs of vacuum amount dependences $p_{2v} = p_a - p_2$ and $p_{1v} = p_a - p_1$, which

are formed by ejector in radial groove 14 and suction hole 2, from radial clearance are given in Figures 5 and 6.

As it may be seen in Figure 4, the width of negative pressure zones on the OM surface and their numerical values essentially depend on design of the hard suction cup. For instance, Bernoulli–vacuum gripping devices which have radial groove 14 increase the width of negative pressure zone. Therefore, they will provide more lifting force. When using capillary tube restrictor or having a shift δ between surface butt ends (Figure 4), numerical values of negative pressure in the radial groove 14 (Figure 5) decrease. However, a possibility of OM non-contacting holding is preserved.

Amount of vacuum formed by ejector in the radial groove 14 and suction hole 2 most of all depends on the radial clearance value (Figures 5 and 6). When $h_0 < 0.01$ mm, negative pressure reaches maximum values, and when $h_0 = 0.1$ mm, it is 10%–20% from maximum values.

Components F_1 , F_2 and resulting lifting force F were calculated using equations (1) and (19) and above-mentioned method.¹⁵ The graphs of dependence of these forces from the value of radial clearance h_0 are shown in Figures 7 and 8. They were calculated with excess pressure of ejector power supply and Bernoulli devices $p_{0\text{ex}} = 300$ kPa and different types of suction cups with the following parameters: $r_0 = 25$ mm, $r_1 = 26$ mm, $r_2 = 30$ mm, $r_3 = 40$ mm, $d_{\text{en}} = 1$ mm, $d_{\text{eb}} = 2$ mm, $l_{\text{eb}} = 8$ mm, $\mu_{\text{en}} = 0.92$, $\lambda_{\text{eb}} = 0.035$, radius of the nozzle BGD $r_n = 1$ mm and radius of the butt end BGD $r_{\text{ef}} = 12$ mm.

Figures 7 and 8 show that the radial groove 14 in suction cup increases OM lifting force. However, if restrictor 13 is

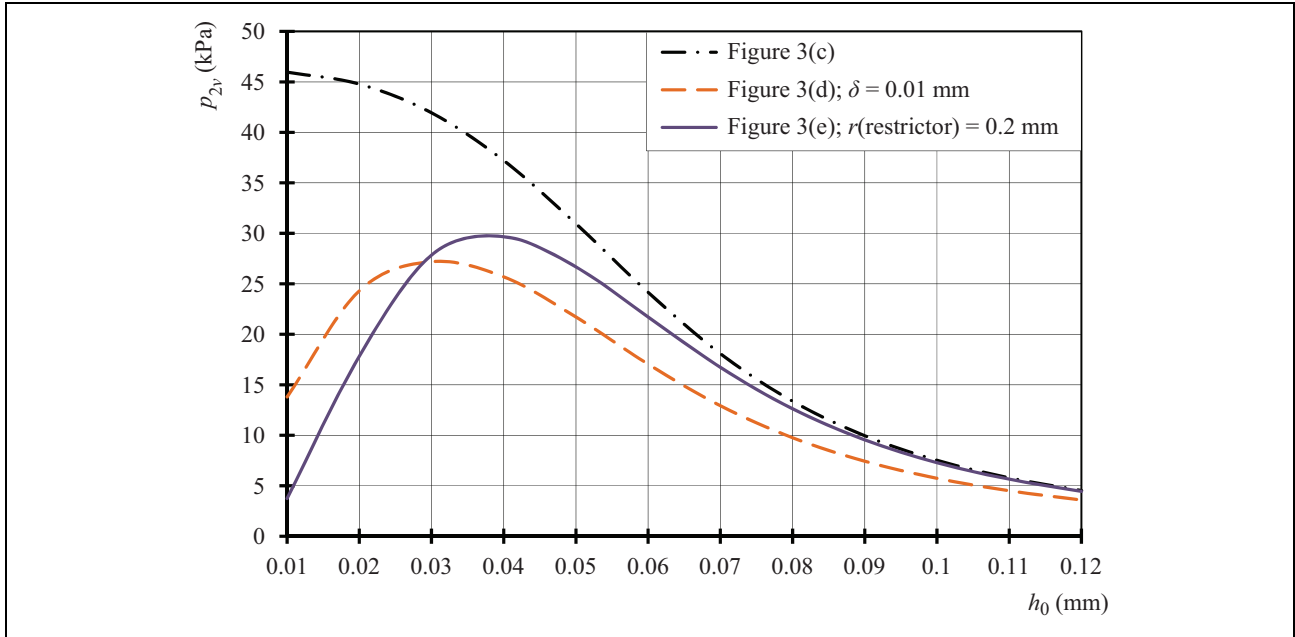


Figure 5. The vacuum amount dependences in the radial groove 14 of suction from radial clearance h_0 for grippers with different suction cup design parameters ($p_{0ex} = 300$ kPa).

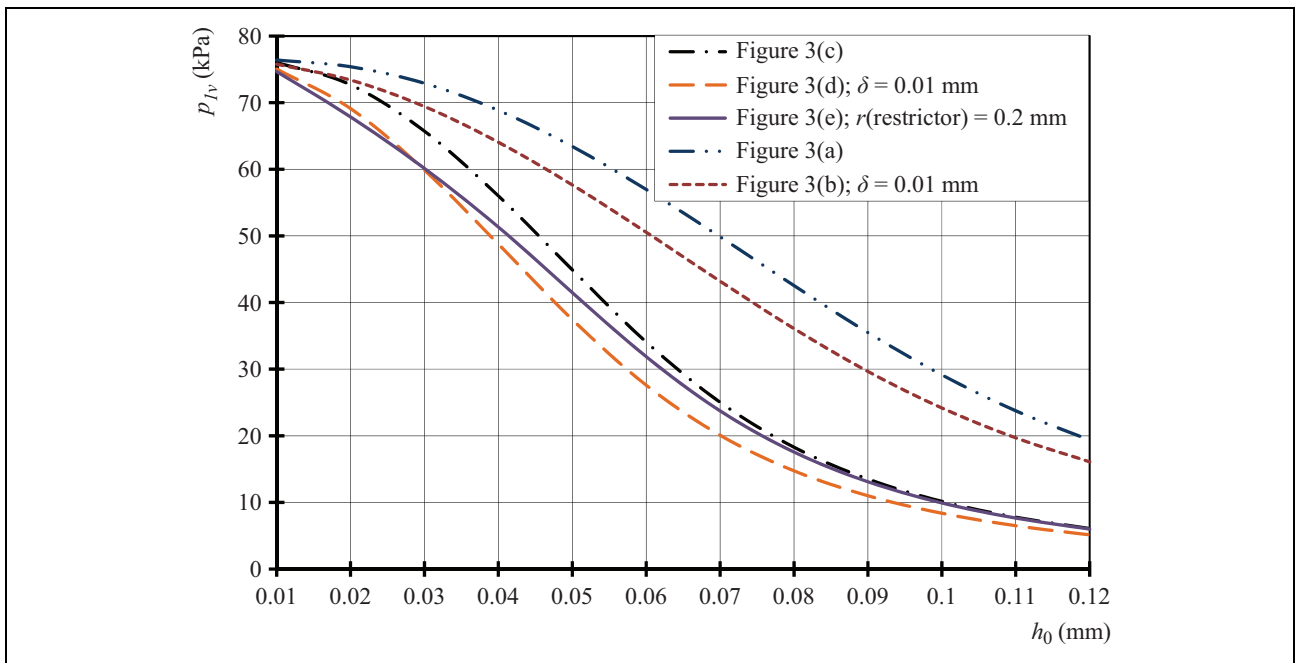


Figure 6. The dependence of vacuum values formed by ejector in the suction hole 2 from radial clearance h_0 for grippers with different suction cup design parameters ($p_{0ex} = 300$ kPa).

additionally used in the suction cup with a radial groove 14 or it has a shift δ between surface butt ends, it leads to the decrease in lifting force approximately for 30%. In this regard, possibility of non-contacting holding of OM even without the use of Bernoulli devices 9 is provided. In this case, optimal value of radial clearance is obtained when $h_0 = 0.02\text{--}0.04$ mm (Figure 7).

The use of Bernoulli devices 9 in given device provides shock-free gripping of the objects, just like when $h_0 < 0.08$ mm between surface butt ends of Bernoulli devices and the OM, and three resilient pneumatic cushions are created. Such combination provides gripping of OM from larger distance and reliable non-contacting holding in the process of manipulation. If suction cup and Bernoulli devices'

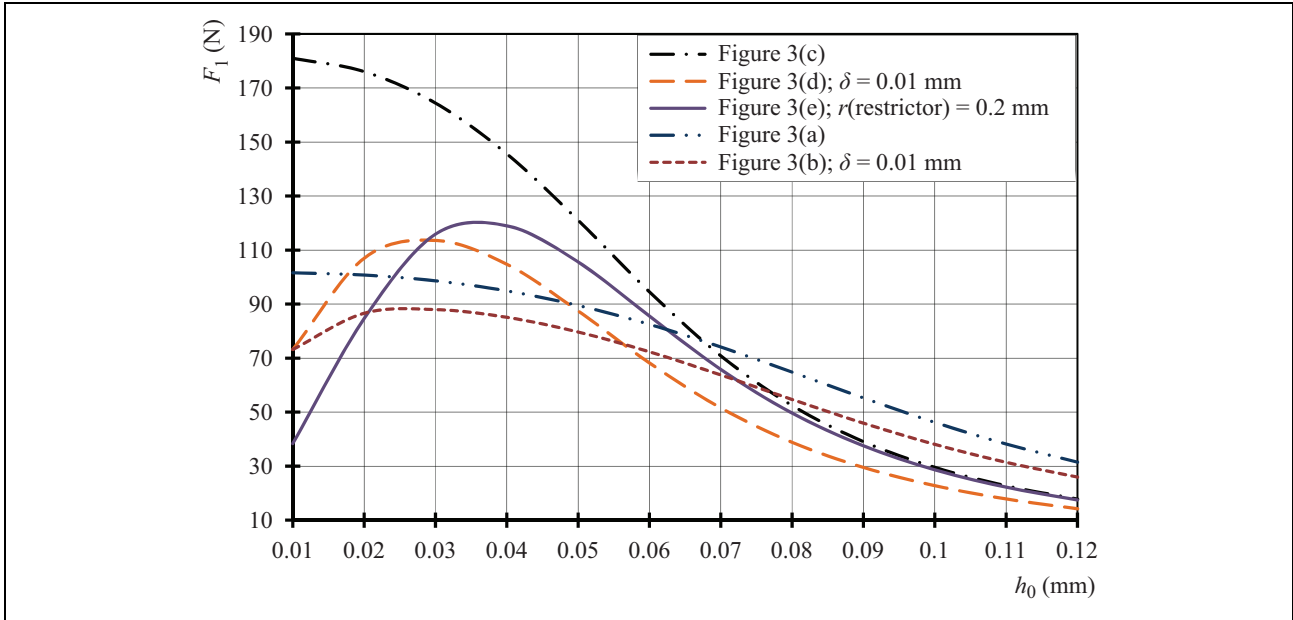


Figure 7. The dependence of force component F_1 from radial clearance h_0 for grippers with different suction cup design parameters.

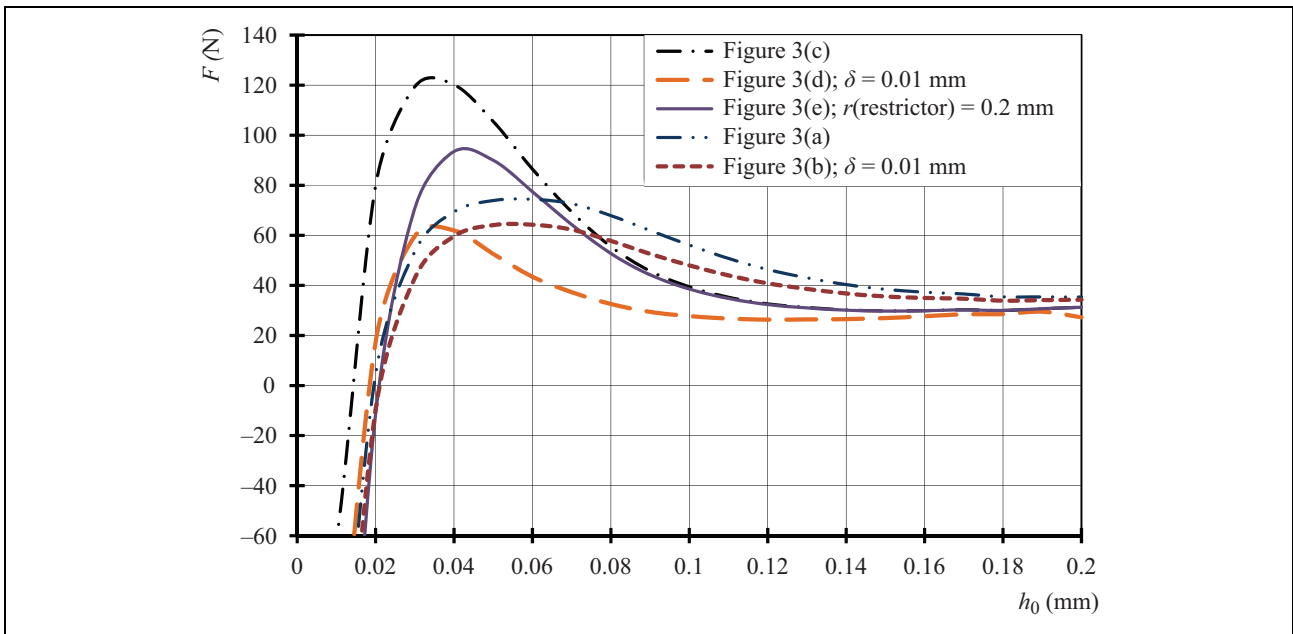


Figure 8. The dependence of resulting force F from radial clearance h_0 for grippers with different suction cup design parameters.

surface ends are on the same flat surfaces, the maximum suction force of parts by multiple-unit gripper is shown in spaces $h_1 = 0.04–0.06$ mm.

To determine the advantages and disadvantages (Table 1) of Bernoulli–vacuum grippers with different designs of suction cup (Figure 3), the following parameters were analyzed: maximum lifting capacity, maximum distance where OM from certain weight may be gripped and working value (equal to stable value of gripped OM) of radial clearance.

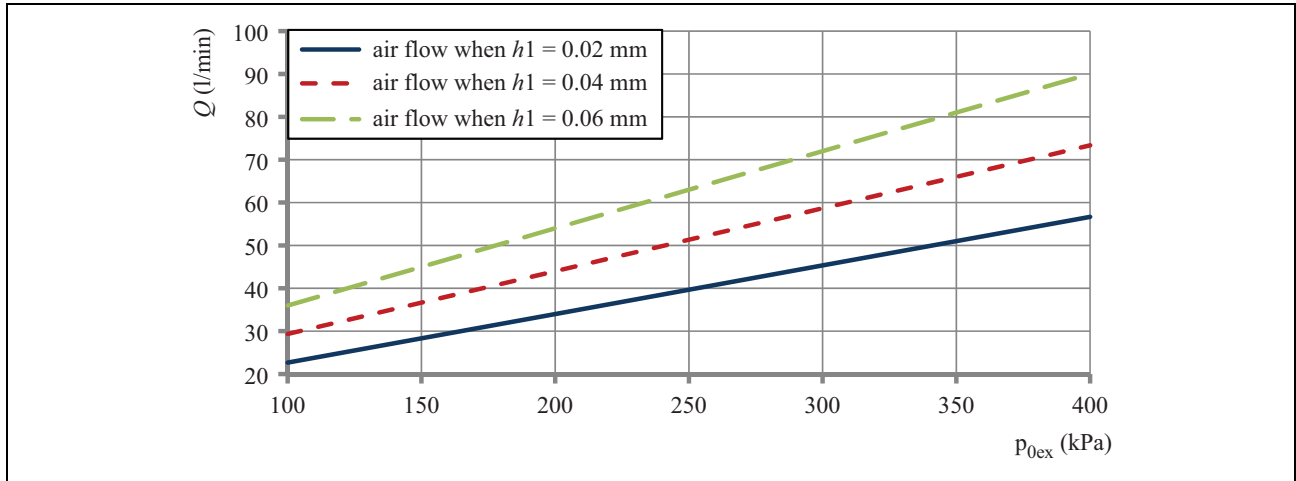
So, to provide maximum lifting capacity, according to Figure 3(c), suction cup should be used. If it is required to grip OM from larger distance, according to Figure 3(a), the suction cup should be used. Suction cup design, according to Figure 3(e), is the most satisfying one. Suction cup design, according to Figure 3(d), has the worst characteristics, that’s why it is unreasonable.

The total mass flow rate of air consumed by the Bernoulli–vacuum gripping device (Figure 9) is calculated using the equation $G = G_e + 3G_{bv\text{gd}}$, where $G_{bv\text{gd}}$ is the

Table 1. Advantages and disadvantages of Bernoulli–vacuum gripping devices with different suction cup designs.

Suction cup design	Characteristics of Bernoulli–vacuum gripping devices (high values +/low values –)		
	Lifting capacity	Distance of OM gripping	Working radial clearance
Figure 3(a)	–	++	+
Figure 3(b)	–	+	+
Figure 3(c)	++	+	–
Figure 3(d)	–	–	–
Figure 3(e)	+	+	+

OM: object of manipulation.

**Figure 9.** Dependence of the capacity flow of air on the pressure of the supply.

mass flow rate of air consumed by one BGD. In accordance with equation (8), we obtain

$$G = \pi \left(\mu_{\text{en}} \frac{d_{\text{en}}^2}{4} + 6\mu_{\text{bg}} r_n h_1 \right) p_0 \sqrt{\frac{2}{RT_a} \frac{k}{k+1} \left(\frac{2}{k+1} \right)^{\frac{2}{k-1}}} \quad (20)$$

where $\mu_{\text{bg}} = 0.78\text{--}0.82$ is the air flow rate through the nozzle of the BGD.

The total volume of air flow is brought to normal conditions $Q = G/\rho_a$, where $\rho_a = 1293 \text{ kg/m}^3$ is the density of air under normal conditions.

The indicator of the noise characteristics of the Bernoulli–vacuum gripping device is the level of sound that appears when the compressed air flows from the nozzle of gripper and the exhaust chamber of the ejector. At pressures of power supply of the Bernoulli–vacuum gripping device to 300 kPa, the noise does not exceed the sound level of 90 dB, which corresponds to the sanitary norms. If there is an object at the end of the Bernoulli–vacuum gripping device, the noise level is reduced. To reduce noise at the output of the ejector, silencer should be used.

The Bernoulli–vacuum gripping device is used for contactless holding of manipulation objects with a surface sensitive to damage, for example object manipulation of fragile material or objects that have different coverage.

Conclusion

Mathematical models that allow to determine the distribution of negative pressure on the surface of OM and power characteristics of Bernoulli–vacuum gripping device were proposed.

On the basis of the conducted modeling, the influence of the design parameters of the vacuum suction cup on the performance characteristics of the Bernoulli–vacuum grippers was established. The performance of characteristics of Bernoulli–vacuum gripping device was investigated.

Reasonable designs of vacuum suction cups are presented and their parameters are explained, which will allow to increase lifting capacity of Bernoulli–vacuum grippers or to decrease compressed air flows.

Declaration of conflicting interests

The author(s) declared no potential conflict of interest with respect to the research, authorship and/or publication of this article.

Funding

The author(s) disclosed receipt of the following financial support for the research, authorship, and/or publication of this article: This work was supported by Slovak National Grants Req-00347-0001, VEGA 1/0065/16, APVV-16-0006 and VEGA 1/0752/17.

References

1. Kozyrev Y. *Gripping devices and industrial robots' tools*. Moscow: Knorus, 2011. (in Russian: Zakhvatnye ustroystva instrumenty promyshlennykh robotov).
2. Ozcelik B, Erzincanli F and Findik F. Evaluation of handling results of various materials using a non-contact end-effector. *Ind Robot Int J* 2003; 30(4): 363–369.
3. Ozcelik B and Erzincanli F. Examination of the movement of a woven fabric in the horizontal direction using a non-contact end-effector. *Int J Adv Manuf Technol* 2004; 25(5–6): 527–532.
4. Davis S, Gray J and Caldwell D. An end effector based on the Bernoulli principle for handling sliced fruit and vegetables. *Robot Comput Int Manuf* 2008; 24(2): 249–257.
5. Bosch Rexroth AG. The drive & control company—Bosch Rexroth AG. *Boschrexroth.com*, 2017. <https://www.boschrexroth.com/en/xc/home/index> (accessed 14 October 2017).
6. Vacuum Components, Floating Suction Pads SBS. *Millsom.com.au*, 2017. <http://www.millsom.com.au/products/vacuum-components/special-grippers/sbs> (accessed 14 October 2017).
7. SMC Products. *Smcworld.com*, 2017. http://www.smcworld.com/products/en/vacuum/s.do?ca_id=1036 (accessed 14 October 2017).
8. Festo - Support Portal - Bernoulli gripper OGGB. *Festo.com*, 2017. https://www.festo.com/net/sv_se/SupportPortal/default.aspx?cat=4564 (accessed 14 October 2017).
9. End Effectors - Mechatronic Systemtechnik GmbH. *Mechatronic.at*, 2017. <http://www.mechatronic.at/technology/end-effectors.html> (accessed 14 October 2017).
10. Stühm K, Tornow A, Schmitt J, et al. A novel gripper for battery electrodes based on the Bernoulli-principle with integrated exhaust air compensation. *Procedia CIRP* 2014; 23: 161–164.
11. Shi K and Li X. Optimization of outer diameter of Bernoulli gripper. *Exp Therm Fluid Sci* 2016; 77: 284–294.
12. Li X and Kagawa T. Theoretical and experimental study of factors affecting the suction force of a Bernoulli gripper. *J Eng Mech* 2014; 140(9): 04014066.
13. Sam R and Nefti S. A novel, flexible and multi-functional handling device based on Bernoulli principle. In: *IEEE International Conference on System Engineering and Technology (ICSET)*, Shah Alam, 27–28 June 2011, pp. 166–171. doi: 10.1109/ICSEngT.2011.5993443.
14. Dini G, Fantoni G and Failli F. Grasping leather plies by Bernoulli grippers. *CIRP Annal* 2009; 58(1): 21–24.
15. Prots Y and Savkiv V. Gas-dynamic analysis of Bernoulli devices for flat blanks. In: *Optimization of industrial processes*. Sevastopol: SevGTU Editor Kopp V.Ya., Vol. 1, 1999, pp. 63–68. (in Russian: Gazodinamicheskii analiz struinykh zakhvatov ploskikh zagotovok).
16. Idel'chik I. *Flow friction manual*. Mashynostroyeniye, 1992. (in Russian: Idel'chik, I. E. (1992). Spravochnik po gidravlicheskim soprotivleniyam; pod redaktsiyei MO Shteynberga, Handbook of hydraulic resistance; ed. by MO Shteynberg. Moscow, Mashinostroenie Publ.).
17. Fedorets V, Pedchenko M and Strutynskyi V. *Hydraulic drive and hydraulic and pneumatic control systems*. Edited by Fedorets. Kyiv: Vyshchashkola, 1995. (in Ukrainian: Hidropryvody ta gidropnevmoavtomatyka).
18. Savkiv V and Prots Ya. Bernoulli devices for “flange” type objects. *Sci J Ternopil Nation Tech Univ* 1998; 3(4): 120–124. (in Ukrainian: Strumenevi zakhopliuuchi prystroi ob'ektiv typu “flantsi”).